Differential Dynamic Modulus of Polyisobutylene with High Molecular Weight. 1. Single-Step Large Shearing Deformations

Yoshinobu Isono,* Kenji Itoh, Toshio Komiyatani, and Teruo Fujimoto

Department of Materials Science and Technology, Nagaoka University of Technology, Nagaoka, Niigata 940-21, Japan

Received September 17, 1990; Revised Manuscript Received March 11, 1991

ABSTRACT: The relaxation shear modulus was measured at 20 °C for polyisobutylene whose viscosity-average molecular weights ranged from 9.6×10^5 to 1.5×10^6, at shear strain (γ) from 0.1 to 4.0, over a time scale from 10 to 10^5 s. In a long-time region, the relaxation modulus $G(\gamma;t)$ could be expressed by the product $G(0;t)h(\gamma)$. The observed $h(\gamma)$ agreed well with the theory of Doi–Edwards without use of IA approximation. Simultaneous measurements of the differential storage and loss moduli, $G'(\omega,\gamma;t)$ and $G''(\omega,\gamma;t)$, were made during the relaxation process with intermittently superposed small sinusoidal oscillations at 0.1 Hz, which falls in the middle of the plateau zone of the polymers. It was confirmed that the total density of entanglement remains constant during the stress relaxation process at small strains, but the entanglement structure changes at large strains. The change and the recovery of the entanglement structure are discussed in terms of the Doi–Edwards theory.

Introduction

In concentrated solutions or melts of linear polymers with high molecular weights, the polymers are entangled with each other, forming a quasi-network structure. The viscoelastic properties of such well-entangled polymers can be expressed by two parameters, for example, the plateau modulus and the maximum relaxation time.[1-6] The former is a measure of the entanglement structure. In linear viscoelasticity, it is a measure of the average entanglement density.

It has been assumed that each molecule is repeating the process of leaving its old constraints and entering a new one. In the range of linear viscoelasticity, the dissolution and re-formation of entanglements are balanced. So the density of entanglement remains constant. This assumption was experimentally confirmed by measuring the differential dynamic modulus by oscillatory deformations superposed on a small shearing deformation.[7]

For a large step strain, the relaxation modulus depends on strain. However, the maximum relaxation time has been proved to be independent of strain even outside the range of linear viscoelasticity.[8-14] On the other hand, the plateau modulus is not always constant. This may arise from a change in entanglement density[7,15-19] and/or an anisotropic configuration of the chain molecules.[2] The measurements of superposed oscillatory deformations can provide additional information on the change in the entanglement structure.

The purpose of this paper is to show that the entanglement structure really changes with strain in the stress relaxation experiments if the strain is large, by superposing small sinusoidal oscillations at a frequency that falls in the middle of the plateau zone of the polymer.

The most difficult problem in experiments of this kind may be to avoid the slippage of the polymer samples on the surface of the plates. The possibility of slippage has not been taken into account that much, although numerous experiments on stress relaxation in shear have been made. In this work, it was experimentally confirmed in each experiment that there was no detectable slippage between the sample and the plates.

Materials and Methods

Samples of commercial polyisobutylene, L-80, -100, and -120, were generously offered by Exxon Chemicals Company. Their intrinsic viscosities in toluene at 30 °C were 2.0_4, 2.3_5, and 2.7_6 dL/g, respectively, from which the viscosity-average molecular weights were determined[20] to be 9.6×10^5, 1.2×10^6, and 1.5×10^6, respectively. Taking the molecular weight between entanglements, M_e, as 7600, these correspond to values for the number of entanglements per molecule of $N = 1.3 \times 10^2$, 1.6×10^2, and 2.0×10^2, respectively. These samples were used at the undiluted state.

Hollow cylinder-shaped specimens of polyisobutylene with inner and outer diameters of 6 and 10 mm, respectively, were used. When such a cylinder is deformed in torsion, the strain is proportional to the radial distance from the center; the shear strain as reported is calculated at the mean radius, so the extremes differ from this value by approximately ±25%.

To avoid possible slippage between sample and plate, we adopted a special device. Figure 1 shows the method for fixing the sample cylinder. The cylinder-shaped sample was first cemented to the steel plates at the inside with a cyanoacrylate glue. Then the outside was pinched in specially designed steel guides together with use of the glue. The guides were fastened firmly with bolts. Finally, the guides were fixed to the plates with setscrews. The sample height between plates was 1.5–2.5 mm. All the measurements were made at 20 °C.

The apparatus for simultaneous measurements of stress relaxation and differential dynamic modulus was a Weissenberg Rheogoniometer R-18 manufactured by Sangamo Controls Ltd. This apparatus has two independent driving systems; one for rotation and the other for a rotational oscillation; this is suitable for the present experiments.

A static shear was given by rotating the driving shaft quickly by hand with a handle. The given angle of rotation was monitored with a potentiometer set on the axis. In small strain measurements, it was double-checked by measuring the traveling distance of the handle with a micrometer. The static shear strain varied from 0.1 to 4.0. The strain amplitude of the oscillatory deformations was less than 0.03. In this range of oscillatory amplitude, a differential dynamic modulus was found to be independent of the amplitude, even if the static strain was large. The frequency of oscillation was 0.1 Hz, which falls about in the middle of the plateau zone of linear viscoelasticity for the present polymers, as shown later.

Figure 2 shows an example of the side view of the deformed sample for a static shear strain of 1.0. Before shearing, a vertical black ink line was drawn on the outside of the sample cylinder. After torsion, the original vertical ink line tipped, with a uniform slope equal to that calculated from the angular displacement of the lower plate, indicating uniform shear strain at the outer edge of the cylinder.

Figure 3 shows the dynamic modulus and loss tangent master curves for sample L-100 in linear viscoelasticity, where mea-

0024-9297/91/2224-4429$02.50/0

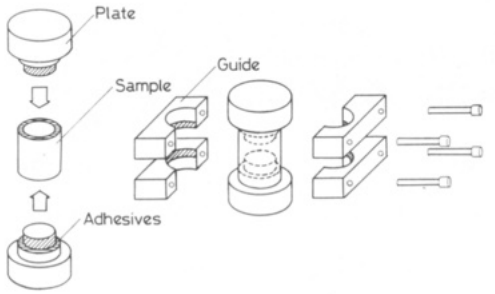

Figure 1. Schematic illustration of the sample form and the procedure for fixing the sample onto the plates.

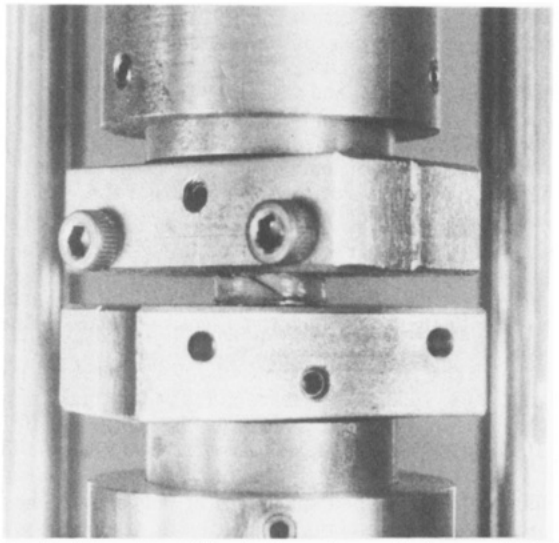

Figure 2. Side view of the deformed sample for $\gamma = 1.0$. The tipped line on the sample is a fiducial mark by black ink to check uniformity in shear strain. This line was vertical before shearing.

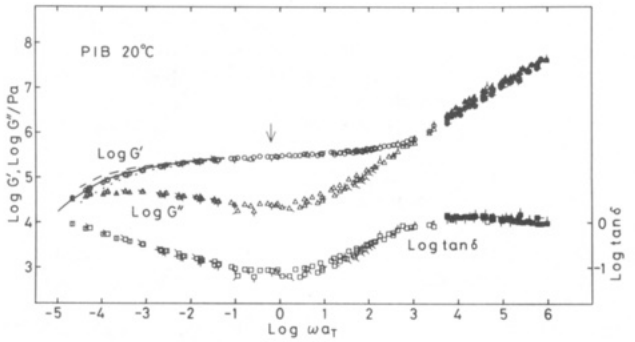

Figure 3. Dynamic modulus and loss tangent master curves for the undiluted polyisobutylene L-100 at 20 °C. Open and filled symbols show the data obtained by tensile oscillatory and shear oscillatory deformations, respectively, where the values of E' and E'' by the former method were converted to G' and G'' by assuming the Poisson ratio $\mu = 0.5$. The solid line denotes the storage modulus converted from the shear relaxation modulus for the same sample. Other dotted and broken lines denote the storage moduli converted similarly for samples L-80 and L-120, respectively. The arrow denotes the frequency of the superposed small oscillations ($\log \omega = -0.2$, $\nu = 0.1$ Hz).

surement temperatures ranged from −41.5 to 186.5 °C and the reference temperature was 20.0 °C. The shift factors, $\log a_T$, fit the WLF equation with the coefficients $C_1 = 9.00$ and $C_2 = 200$, which were very close to the literature values.[21] The solid line in the figure shows the values of $G'(\omega)$ converted from $G(t)$ for the same sample by an approximate equation from linear viscoelasticity theory:[1]

$$G'(\omega) = G(t) + H(\tau)\Psi(m) \qquad \text{at } \omega = t^{-1} \tag{1}$$

where $H(\tau)$ is the relaxation spectrum calculated from $G(t)$ by the well-known approximation relation[1] and $\Psi(m)$ is a numerical

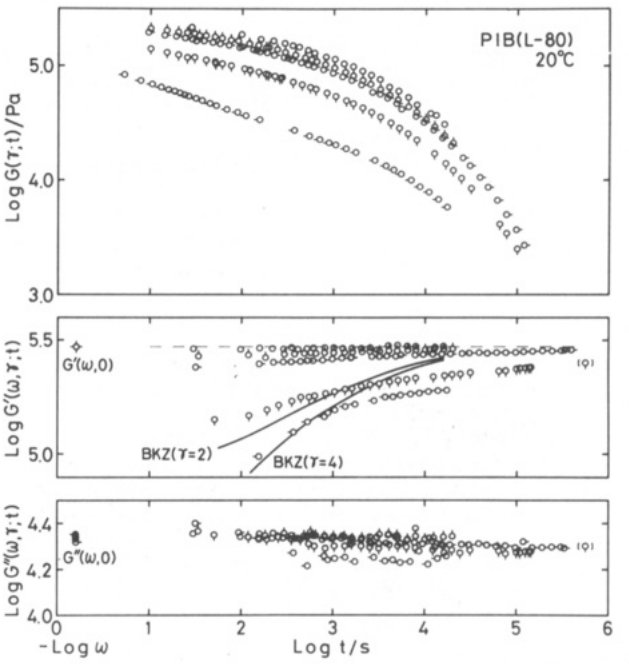

Figure 4. Double-logarithmic plots of $G(\gamma;t)$, $G'(\omega,\gamma;t)$, and $G''(\omega,\gamma;t)$ against t for five different strains. No pip, $\gamma = 0.1$; pip up, $\gamma = 0.5$; successive 90° rotations clockwise, 1.0, 2.0, and 4.0. $G'(\omega,0)$ and $G''(\omega,0)$ denote measurements before imposition of strain, at the frequency shown on the abscissa scale at the left. The solid lines in the middle panel denote predictions of the BKZ theory for $\gamma = 2.0$ and 4.0, respectively, by eq 3.

factor introduced by Catsiff and Tobolsky.[22] The excellent agreement lends considerable confidence to the accuracy of the measurements. Other dotted and broken lines show the converted values of $G'(\omega)$ for samples L-80 and L-120, respectively. The present samples have molecular weight distributions. The heterogeneity factor, M_w/M_n, estimated by GPC on the basis of the calibration curve of standard polystyrenes was 2.1–2.3. However, a very clear rubbery plateau was observed. The arrow in Figure 3 shows the frequency of the superposed oscillations. We note that the present measurements of the differential dynamic modulus are made in the middle of the rubbery plateau zone.

Results

The linear and nonlinear relaxation moduli, represented by $G(0;t)$ and $G(\gamma;t)$, respectively, for sample L-80 are plotted double-logarithmically against time for various strains in the top panel of Figure 4. These curves can be shifted vertically to be superposed at a long-time region as shown in the top panel of Figure 5. Similar results were obtained for the other samples, too. Therefore, $G(\gamma;t)$ can be factored into strain-dependent and time-dependent terms as expected:[2,5,6,8-14]

$$G(\gamma;t) = h(\gamma)G(0;t) \tag{2}$$

However, it cannot be factored in the short-time side, as reported by Osaki et al.[8,9,12] and Larson et al.[14] From the master curve of $G'(\omega)$ in Figure 3, the longest relaxation time in the transition zone, τ_{tr} (which is independent of molecular weight and molecular weight distribution), is estimated to be 3.7×10^{-3} s at 20 °C. If we use this value, the equilibration times in the Doi model,[23] τ_e ($=2N^2\tau_{tr}$), are estimated to be 1.3×10^2, 1.9×10^2, and 3.0×10^2 s for samples L-80, L-100, and L-120, respectively. Osaki has reported for monodisperse polystyrene solutions that the characteristic time, τ_k, after which the strain-dependent relaxation modulus can be written by eq 2, is 4.5 times longer than τ_e. The values of τ_k ($=9N^2\tau_{tr}$) are estimated to be 5.6×10^2, 8.5×10^2, and 1.3×10^3 s, respectively.

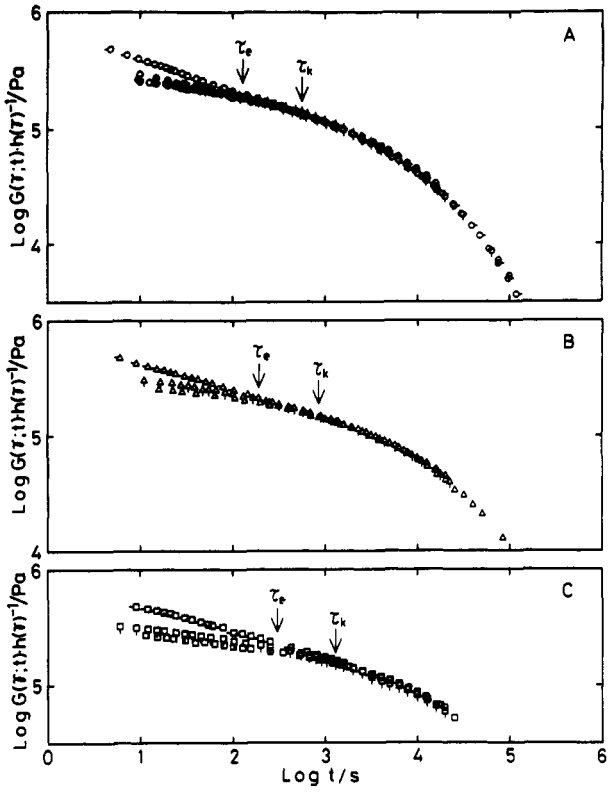

Figure 5. Double-logarithmic plots of reduced relaxation modulus $G(\gamma;t)/h(\gamma)$ against t. (A) Sample L-80; (B) sample L-100; (C) sample L-120. Various directions of pips denote various shear strains; no pip, $\gamma = 0.1$; pip up, $\gamma = 0.5$; successive 90° rotations clockwise, 1.0, 2.0, and 4.0 in all the symbols.

These values, shown by arrows in Figure 5, almost agree with the present data, although the present samples have broad molecular weight distributions.

The differential storage and loss moduli, $G'(\omega,\gamma;t)$ and $G''(\omega,\gamma;t)$, for sample L-80 are plotted double-logarithmically against time in the bottom two panels of Figure 4. The initial values of $G'(\omega,0)$ and $G''(\omega,0)$, measured before being strained in each experiment, are shown at the left of each panel. For the smallest strain, both $G'(\omega,\gamma;t)$ and $G''(\omega,\gamma;t)$ remain practically equal to $G'(\omega,0)$ and $G''(\omega,0)$, respectively, throughout the relaxation process. This is consistent with the previous result,[7] showing that the total density of entanglement remains constant in the linear region.

For the higher strains in Figure 4, the first values of $G'(\omega,\gamma;t)$ obtained about 30–140 s after being strained are much smaller than $G'(\omega,0)$, showing a change in the entanglement structure. The degree of decrement is more remarkable with increasing static strain. The first low values of $G'(\omega,\gamma;t)$ recover gradually with time. For $\gamma = 0.5$ and 1.0, $G'(\omega,\gamma;t)$ substantially attains the original zero-strain value after about 10^4 and 10^5 s, respectively. For the others, $G'(\omega,\gamma;t)$ does not attain the original value even after about 140 ks. In the case of $\gamma = 2$, we raised the temperature to 37 °C for one night, with the expectation that a recovery process would be accelerated at the higher temperature. The values of G' and G'' after the temperature was returned to 20 °C are put in parentheses. However, the difference $\Delta\log G'$ [=log $G'(\omega,0)$ − log $G'(\omega,\gamma;t)$] remained as 0.07. $G''(\omega,\gamma;t)$ shows a small increase followed by a gradual decrease.

Thus, it is certain that the entanglement structure of the polymeric materials changes with the strain given to the material, and the recovery of the structure is slow.

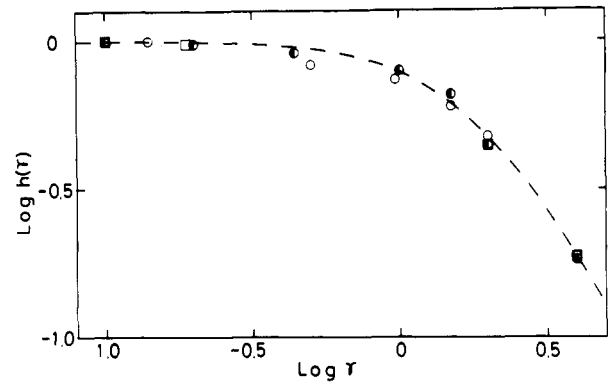

Figure 6. Static shear strain dependence of $h(\gamma)$ determined in Figure 5. Open circle, half-filled circle, and square denote the data for L-80, L-100, and L-120, respectively. The broken line denotes prediction of the Doi–Edwards theory without use of independent alignment approximation.

Discussion

The experimental values of $h(\gamma)$ are plotted double-logarithmically against shear strain in Figure 6. The broken line shows the theoretical values by Doi and Edwards without use of the independent alignment approximation.[2] In the theory, the anisotropy of the chain configuration in the deformed tube is taken into account. Experimental values agree with the theory. Such an agreement for the sample of N (=CM/M_e) < 50 was observed by Osaki et al.,[12] Vrentas and Graessley,[13] and Larson et al.[14] However, they have reported that the experimentally observed $h(\gamma)$ is much lower than the theoretical prediction, if $N > 50$,[13,14,24] despite the fact that the Doi–Edwards theory should be more valid in the higher molecular weight sample. In contrast with their results, our experimental data with the sample of $N > 50$ are in good agreement with the Doi–Edwards theory. It may be concluded that the Doi–Edwards theory is valid at $t \geq \tau_k$.

In the BKZ theory,[25] our aimed differential dynamic modulus can be represented as follows:[26]

$$G'(\omega,\gamma;t) = \frac{\partial\sigma(\gamma;t)}{\partial\gamma} - G(0;t) + G'(\omega,0) \tag{3}$$

$$G''(\omega,\gamma;t) = G''(\omega,0) \tag{4}$$

where $G(0;t)$ is the relaxation modulus in linear viscoelasticity and $\sigma(\gamma;t)$ is the relaxation of stress after imposition of step strain γ. If $\sigma(\gamma;t)$ is separable into strain-dependent and time-dependent terms, eq 3 can be written with $h(\gamma)$.

$$G'(\omega,\gamma;t) = \left(\frac{\partial\gamma h(\gamma)}{\partial\gamma} - 1\right)G(0;t) + G'(\omega,0) \tag{5}$$

Equation 5 is the same as predicted from the Doi–Edwards theory with use of an independent alignment approximation.

In the linear viscoelasticity, $G'(\omega,\gamma;t)$ is reduced to $G'(\omega,0)$. Equation 3 predicts that $G'(\omega,\gamma;t)$ is smaller than $G'(\omega,0)$ at finite times and attains $G'(\omega,0)$ at infinite time, in qualitative agreement with the present experimental results. Solid lines in the middle panel of Figure 4 show the calculated values of $G'(\omega,\gamma;t)$ for $\gamma = 2.0$ and 4.0, respectively. The calculated values agree fairly well with the observed one in the short-time region, though the rate of structure recovery predicted by the theory is too high in the long-time region ($t > \tau_k$). Thus, the values of $h(\gamma)$ can be explained well by the Doi–Edwards theory, but the

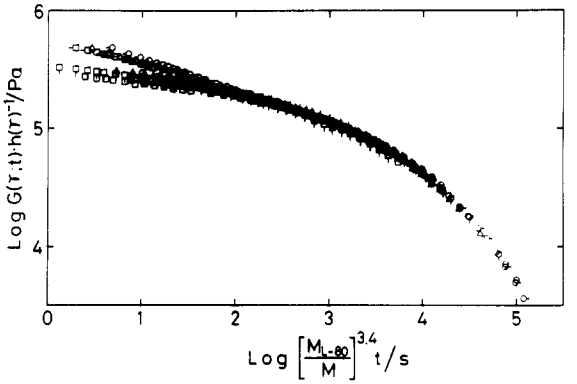

Figure 7. Double-logarithmic plots of reduced relaxation modulus $G(\gamma;t)/h(\gamma)$ against $(M_{L\text{-}80}/M)^{3.4}t$ for all the samples, where $M_{L\text{-}80}$ and M denote the molecular weight of the sample L-80 and the individual sample, respectively. Symbols are the same as in Figure 5.

values of $G'(\omega,\gamma;t)$ calculated from eq 5 with the values of $h(\gamma)$ do not agree with the experimental results at long times. The fact that the observed $G'(\omega,\gamma;t)$ is lower than the predicted curve of eq 5 at $t > \tau_k$ may mean that the entanglement structure does not always attain the equilibrium structure even if the stress relaxes. Furthermore, the fair agreement of the predicted $G'(\omega,\gamma;t)$ with the observed one at $t < \tau_k$ may imply that the nonlinearity of $G(\gamma;t)$ in this time region is due to the change in entanglement structure.

An explanation of the drop in $G'(\omega,\gamma;t)$ followed by recovery may be possible on the basis of the Doi theory.[23] As discussed in a previus paper,[7] one may postulate that entanglements are lost by equilibration, as each molecule shrinks in its "tube" with a time scale τ_e and is regained in relaxed configurations by disengagement with a time scale τ_d. Such an idea can be tested by plotting the data against t/τ_e and also against t/τ_m, where τ_m is the maximum relaxation time. In the present measurements, a complete terminal zone could not be attained because of the very high molecular weights of the samples. However, the maximum relaxation time is expected to depend on $M^{3.4}$, because all the relaxation modulus data can be reduced by a factor of $M^{3.4}$ at long times as shown in Figure 7. τ_e is expected to depend on M^2. So the data of $G'(\omega,\gamma;t)$ for $\gamma = 2$ and 4 are plotted double-logarithmically against $(M_{L\text{-}80}/M)^{3.4}t$ and $(M_{L\text{-}80}/M)^2t$ in Figure 8, where $M_{L\text{-}80}$ is the molecular weight of sample L-80. As expected, the reduction is somewhat less successful at short times in Figure 8A and at long times in Figure 8B, although the differences are slight. A better interpretation could be achieved with a broader range of molecular weights and narrower molecular weight distributions. In any case, the results are consistent with the expected behavior of τ_e and τ_d.

Acknowledgment. A part of this work was supported by the Saneyoshi Scholarship Foundation. We are greatly indebted to Professor John D. Ferry of the University of Wisconsin and Professor Mitsuru Nagasawa of the Toyota Institute of Technology for their valuable comments.

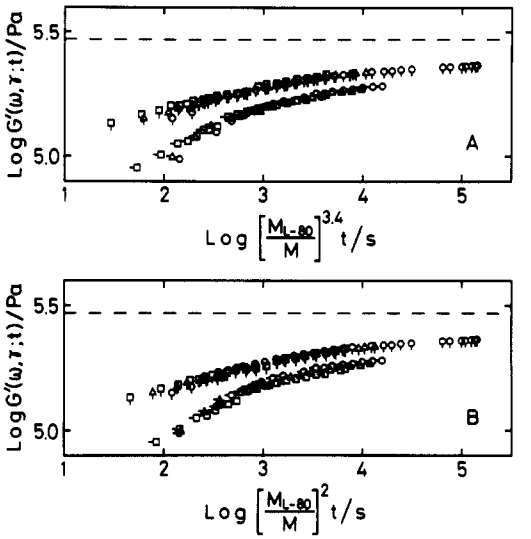

Figure 8. Double-logarithmic plots of $G'(\omega,\gamma;t)$ against $(M_{L\text{-}80}/M)^{3.4}t$ (A) and $(M_{L\text{-}80}/M)^2t$ (B) for two different static shear strains $\gamma = 2.0$ and 4.0. Symbols are the same as in Figure 5. The broken line denotes the value of $G'(\omega,0)$.

References and Notes

(1) Ferry, J. D. *Viscoelastic Properties of Polymers*, 3rd ed.; Wiley: New York, 1980.
(2) Doi, M.; Edwards, S. F. *J. Chem. Soc., Faraday Trans. 2* **1978**, *74*, 1789, 1802, 1818; **1979**, *75*, 38.
(3) Curtiss, C. F.; Bird, R. B. *J. Chem. Phys.* **1981**, *74*, 2016, 2026.
(4) Graessley, W. W. *Adv. Polym. Sci.* **1974**, *16*, 1.
(5) Graessley, W. W. *Adv. Polym. Sci.* **1982**, *47*, 67.
(6) Osaki, K. In *Molecular Conformation and Dynamics of Macromolecules in Condensed Systems*; Nagasawa, M., Ed.; Elsevier: Amsterdam–Oxford–New York–Tokyo, 1988; p 175.
(7) Isono, Y.; Ferry, J. D. *J. Rheol.* **1985**, *29*, 273.
(8) Einaga, Y.; Osaki, K.; Kurata, M.; Kimura, S.; Yamada, Y.; Tamura, M. *Polym. J.* **1973**, *5*, 91.
(9) Fukuda, M.; Osaki, K.; Kurata, M. *J. Polym. Sci., Polym. Phys. Ed.* **1975**, *13*, 1563.
(10) Laun, H. M. *Rheol. Acta* **1978**, *17*, 1.
(11) Wagner, M. H. *Rheol. Acta* **1979**, *18*, 33.
(12) Osaki, K.; Nishizawa, K.; Kurata, M. *Macromolecules* **1982**, *15*, 1068.
(13) Vrentas, C. M.; Graessley, W. W. *J. Rheol.* **1982**, *26*, 359.
(14) Larson, R. G.; Khan, S. A.; Raju, V. R. *J. Rheol.* **1988**, *32*, 145.
(15) Sakai, M.; Fujimoto, T.; Nagasawa, M. *Macromolecules* **1972**, *5*, 786.
(16) Kajiura, H.; Sakai, M.; Nagasawa, M. *Trans. Soc. Rheol.* **1974**, *18*, 323; **1976**, *20*, 575.
(17) Isono, Y.; Nagasawa, M. *Macromolecules* **1980**, *13*, 862.
(18) Takahashi, Y.; Isono, Y.; Noda, I.; Nagasawa, M. *Macromolecules* **1986**, *19*, 1217.
(19) Takahashi, Y.; Isono, Y.; Noda, I.; Nagasawa, M. *Macromolecules* **1987**, *20*, 153.
(20) Fox, T. G.; Flory, P. J. *J. Phys. Colloid Chem.* **1949**, *53*, 197.
(21) Ferry, J. D. Ref 1, p 606.
(22) Catsiff, E.; Tobolsky, A. V. *J. Colloid Sci.* **1955**, *10*, 375.
(23) Doi, M. *J. Polym. Sci., Polym. Phys. Ed.* **1980**, *18*, 1005.
(24) Osaki, K.; Kurata, M. *Macromolecules* **1980**, *13*, 671.
(25) Bernstein, B.; Kearsley, E. A.; Zapas, L. J. *Trans. Soc. Rheol.* **1963**, *8*, 391.
(26) Isono, Y.; Ferry, J. D. *Rubber Chem. Technol.* **1984**, *57*, 925.